PCCP

ROYAL SOCIETY OF CHEMISTRY

PAPER

Published on 09 October 2026
Licensed under CC-BY-NC 4.0

Check for updates

Cite this: DOI: 10.1039/d6cp03024f

Expanding the polarizing agent toolbox for liquid-state dynamic nuclear polarization: stability and performance at 14.1 T

Kiera Powers, †[a] Daphne Broerman, †[a] John Cerritelli, [b] Sanyog Kumari, [c] Snorri Th. Sigurdsson, [c] Linda H. Doerrer [b] and Tomas Orlando *[a]

Received 2nd August 2026,
Accepted 7th October 2026

DOI: 10.1039/d6cp03024f

rsc.li/pccp

Dynamic nuclear polarization (DNP) in liquids is emerging as a potential technique to increase the NMR signal of routine NMR spectroscopy at high magnetic fields. Monoradicals are utilized as polarizing agents and microwave irradiation is used to transfer the high electron spin polarization to nuclei on nearby molecules. Recently, narrow-line radicals have gained significant interest as polarizing agents because they can efficiently polarize a broad set of nuclei (^{1}H, ^{13}C, ^{19}F, ^{31}P) in various systems, such as neat liquids, viscous liquids, and heterogeneous media. However, these radicals can be unstable in solutions, which can make data reproducibility difficult. Here, we studied the persistence of narrow-line radicals in organic solvents typically used as matrices in liquid DNP. We observed that the persistence of monoradicals varies significantly depending on the monoradical, the solvent, and the storage condition of the sample. Our results aim to serve as a guideline for sample preparation and data reproducibility. Furthermore, we expand the viable class of polarizing agents by introducing two radicals that are new in the context of DNP in liquids driven by the Overhauser effect at high magnetic fields; verdazyl and tris(pentafluorophenyl)methyl (PF-trityl). Our ^{19}F-DNP experiments at 14.1 T show that PF-trityl can polarize aromatic and aliphatic fluorinated molecules equally well, a feature that has not yet been reported and that may be ascribed to the fluorination of the radical itself.

Introduction

Dynamic nuclear polarization (DNP) in liquids has recently attracted renewed attention due to its potential for use as an effective method to increase NMR signal for routine spectroscopy experiments at high magnetic fields ($>$9.4 T).[1–5] The method relies on intermolecular electron–nuclear relaxation mechanisms enabled by microwave irradiation.[6,7] Recent results have shown how DNP is effective on enhancing NMR signals of a variety of NMR active nuclei (^{1}H, ^{13}C, ^{15}N, ^{19}F, ^{31}P).[3,4,8–12] DNP can be applied to small molecules in liquids,[3–5,12] and also to viscous systems,[13,14] such as lipid membranes,[15,16] and heterogeneous media to investigate liquid–solid interfaces.[17,18]

In a standard DNP experiment in liquid, an organic radical is dissolved in an organic solvent—usually non-polar due to their favorable microwave propagation properties[19]—at concentrations in the range 10–40 mM, and in some cases up to 100–200 mM.[8,20] While often the solvent has been used as a primary target for the spin polarization transfer, additional solutes can be added to the mixture, typically with concentrations of $\sim$0.5–1.0 M, to serve as targets. Those are often small molecules,[4,21] drugs,[12] metabolites,[4,11] or catalysts.[17] In these cases, the intermolecular spin polarization transfer between the unpaired electron spins and the nuclear spins is driven by microwave irradiation and enabled by electron–nuclear cross relaxation, a mechanism known as Overhauser effect (OE).[22,23] In conditions of high magnetic field ($\geq$9.4 T) and high microwave power, the solid effect (SE) may also be active in liquids, which allows for the hyperpolarization of larger molecules such as lipid bilayers, peptides, and ATP in viscous media.[13–15] Both OE-DNP and SE-DNP involve transitions between one electron spin ensemble and one nuclear spin ensemble, and therefore are active when using monoradicals instead of biradicals.

Among the monoradicals that have been used in the context of DNP in liquids, BDPA, galvinoxyl and trityl have recently lead to large enhancements at high magnetic fields on some classes of molecules, like aromatic fluorinated compounds,[5,12,24] trivalent phosphorous compounds *via* OE-DNP[17,18,25] and ^{1}H nuclei in viscous matrices through SE-DNP.[13,16] These radicals can be

[a] National High Magnetic Field Laboratory and Florida State University, Tallahassee, Florida, USA. E-mail: torlando@magnet.fsu.edu
[b] Chemistry Department, Boston University, Boston, Massachusetts, USA
[c] Department of Chemistry, University of Iceland, Science Institute, Reykjavik, Iceland
† These authors contributed equally.

categorized as narrow-line radicals, meaning that their EPR line at magnetic fields and radical concentrations typical for DNP ($\geq$9.4 T and 10–40 mM) does not show resolved hyperfine splittings. The resulting single EPR line should favor the saturation of the electronic transitions when irradiating with microwaves at a fixed frequency, therefore leading to higher NMR enhancements.[26,27]

It is well-established that organic radicals degrade over time, especially when dissolved in liquid. This has been recognized also in the context of DNP, where the persistence of radicals in solutions has been reported in water and polar solvents.[28,29] However, the precise extent of this depletion remains largely unquantified in non-polar organic solvents that are commonly used in OE-DNP. Furthermore, different laboratories adopt different practices for sample preparation, storage of the samples, and storage of the radicals themselves, which might affect the persistence of the radical in solution. Consequently, DNP parameters, which are important for disentangling the mechanisms of DNP, might be subject to large variability, obscuring accurate interpretation of the underlying DNP mechanisms.

When considering the factors contributing to the NMR signal enhancements in OE-DNP, the concentration C of the organic radical directly affects all the factors in the Overhauser equation:[22,23] $\varepsilon = 1 - s \cdot f \cdot \xi \cdot (\gamma_e/\gamma_n)$, where ε is the enhancement, γ_e and γ_n are the electron and nuclear gyromagnetic ratios, respectively. The leakage factor f depends on the paramagnetic relaxation rate $R_{1,\mathrm{para}}$ which is directly proportional to the concentration of paramagnetic species in solution.[30,31] The saturation factor s depends on the electronic T_2, which scales with C;[32] for radicals with more than one EPR line, an additional term contributes to s, namely $C \cdot K_x$, where K_x is the Heisenberg exchange rate constant, and C is the radical concentration.[26,33] Finally, the coupling factor ξ contains a direct dependency on the concentration of the organic radical in the terms that account for the intermolecular electron–nuclear dipolar interaction.[34,35] An experimental correlation between the enhancement ε and the radical concentration C has been reported,[4,13] and shows an increase of enhancements with C up to 100 mM, although it largely depends on the sample and the chemical group that is polarized. As a downside, the NMR linewidth deteriorates with increasing radical concentrations, and typical OE-DNP experiments are now conducted with C = 10–40 mM to preserve NMR resolution. Despite these experimental observations, the complex interplay among the parameters in the Overhauser equation prevents a straightforward functional relationship between ε and C.

In this manuscript, we assess, *via* electron paramagnetic resonance (EPR), the persistence of narrow-line organic monoradicals used as polarizing agents (PAs) for DNP in liquids. Our results provide a benchmark on sample preparation protocols and storage that can be useful in the context of quantitative DNP in liquids and may help the community in optimizing the experimental conditions in order to maximize NMR enhancements.

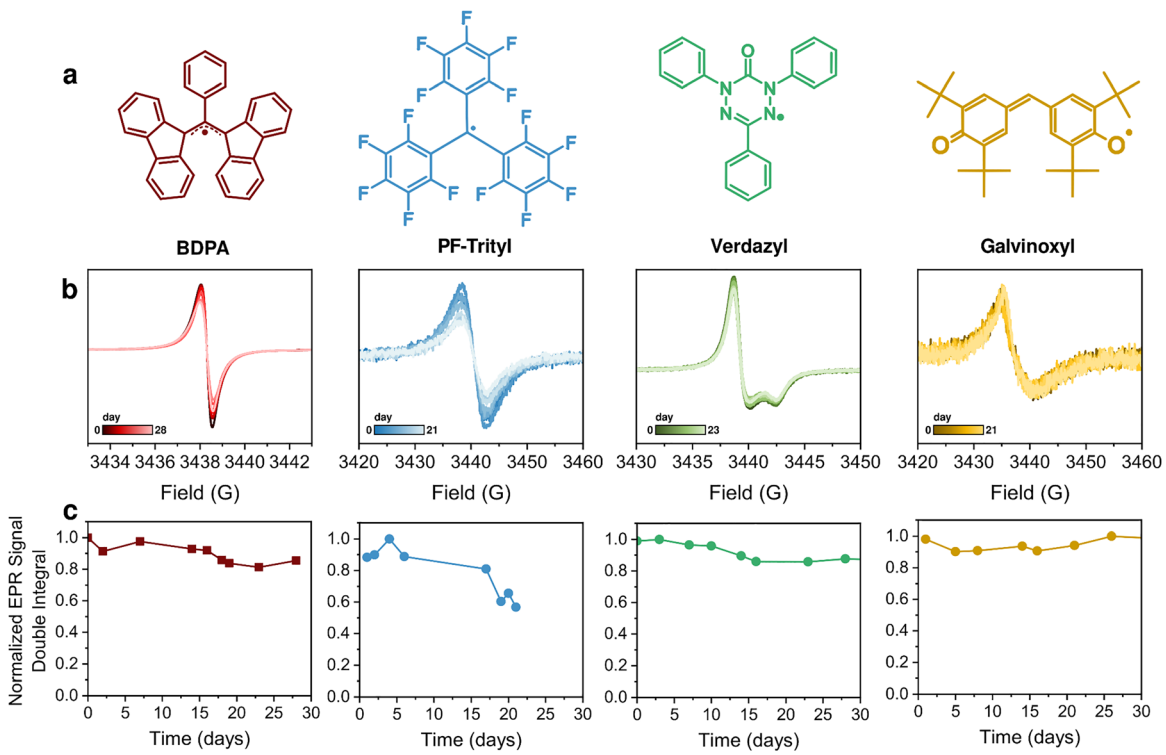


Fig. 1 (a) Structures of the organic radicals used in this work. (b) CW-EPR spectra of powder samples recorded at 9 GHz as a function of time. (c) Persistence of organic radicals in powders measured as the double integral of the CW-EPR spectra. All samples were stored at −80 °C in between measurements.

This journal is © the Owner Societies 2026

Furthermore, we expand the class of PAs for high field OE-DNP in liquids by introducing two monoradicals that are new in this context (Fig. 1), namely (i) fluorinated-trityl (PF-trityl); and (ii) verdazyl. Our ^{19}F-OE-DNP results at 14.1 T show that PF-trityl, unlike other carbon-based radicals, is uniquely capable of effectively polarizing both aromatic and aliphatic fluorinated molecules. We hypothesize that the fluorination of the radical itself may affect the polarization transfer mechanisms.

Materials and methods

Radicals and solvents

The radicals utilized in this study are shown in Fig. 1. BDPA radical (α,γ-bisdiphenylene-β-phenylallyl), TEMPO radical, and galvinoxyl radical were purchased from Sigma Aldrich and used as received. BDPA radical is sold in a 1 : 1 complex with benzene. Compounds were stored as indicated by the manufacturer, unless stated otherwise.

PF-trityl was synthesized using an improved procedure from the existing method,[36] similarly starting with alcohol $HOC(C_6F_5)_3$. Complete details of synthesis will be reported in a forthcoming publication. PF-trityl powder was stored in an air-tight flask under vacuum and inside a −80 °C freezer. Similar polyfluorinated trityl radicals with varying degrees of chloro- and bromo-substituents have been investigated for their luminescent properties.[37] The perfluorotrityl cation, $\{C(C_6F_5)_3\}^+$, has been studied for its super-electrophilicity and ability to abstract a hydride from alkanes.[38–41]

Verdazyl (1,3,5-triphenyl-6-oxoverdazyl) was prepared according to Milcent's procedure[42] with some modifications (SI). Verdazyl powder was stored in a −80 °C freezer.

Organic solvents CCl_4, $CHCl_3$, *p*-xylene and benzene, and the compound triphenylphosphine (PPh_3) were used as received.

Sample preparation

To study the persistence of the radicals in powder, a small amount of sample (∼1 mg) was inserted in a glass capillary and sealed with sealing paste.

Solutions were prepared by mixing the radicals and the solvents. Radical concentrations were chosen as 10–40 mM, compatible with concentrations typically used in DNP experiments. Solutions were sonicated for 2–4 minutes to solubilize the radical as needed. For testing the persistence of the radical over time, 10–30 μL of the same stock solution was transferred into fluorinated ethylene propylene (FEP) tubes (3 mm OD, 1 mm ID). Sample degassing either *via* freeze–pump–thaw cycles, freeze–thaw cycles, or aided by the use of glovebox is a standard practice utilized in DNP for both solids and liquids to remove the O_2 molecules dissolved in the sample. In fact, dissolved O_2 broadens the EPR line, contributes to the paramagnetic relaxation, and ultimately reduces the DNP enhancement. To comply with the standard DNP practices, all samples, unless otherwise specified, were degassed with freeze–pump–thaw cycles (6 to 10 cycles). The vacuum during the pumping phase was provided by a rotary pump reaching 10^{-2}–10^{-3} mbar at the pump inlet. Once degassed, the samples with the degassing manifold were transferred in a glovebox where the tubes were sealed with a hot blade and checked for leaks.

For DNP experiments, samples were 70 μL in volume in FEP tubes, 3 mm OD.[9] All DNP samples were degassed with 6–10 freeze–pump–thaw cycles.

Although FEP tubes are partially porous to O_2 over an extended period of time (>3 weeks),[5] they are a cost effective alternative to quartz tubes, and are easier to handle and seal. More importantly, they offer advantages in terms of microwave propagation when performing DNP at high frequency due to the low refractive index of FEP (n = 1.46, compared to n = 2.04 for quartz).[43]

Sample storage

Within this work, we explored the effect of different storage methods on the radical persistence. Samples were stored under three different conditions, which are labeled as follows: (i) *bench*: sample stored on a laboratory bench at ambient conditions of temperature and light; (ii) *freezer*: sample stored in a −80 °C freezer; (iii) *glovebox*: sample stored in a N_2 glovebox at room temperature.

CW-EPR measurements

Continuous-wave EPR was utilized as a spin counting tool to quantify the radical content in each sample. Measurements were performed with benchtop Bruker EMX nano or with a Bruker Elexys E580, both operating at ∼9.5 GHz/0.34 T. Spectra were recorded with a modulation amplitude of 0.5 G for solutions and 0.032 G for powders, while the modulation frequency was kept at 100 kHz. The measurement parameters were kept consistent for each sample. User error in sample positioning as well as fluctuations in the room temperature account for an error of ∼10%. Spectra were baseline corrected and double integrated with Matlab or Origin.

To estimate the isotropic *g*-value of verdazyl and PF-trityl, we recorded CW-EPR spectra on solution samples at 240 GHz with a heterodyne spectrometer.[44] BDPA was dispersed in the same solution and used as reference (Fig. S3, SI).

Dynamic nuclear polarization

Dynamic nuclear polarization measurements were performed at 14.1 T using a 2-channel probe head equipped with a central waveguide and specifically built to maximize the sample volume (∼70 μL). It allows for decent NMR resolution in the liquid state, down 0.1 ppm in the optimal cases, which corresponds to ∼60 Hz for ^{19}F lines.[5,9] The ^{1}H channel was tuned to 565 MHz to detect ^{19}F resonances. A gyrotron operating at 395 GHz delivers <3 W of microwave power at the sample position.[43,45] The spectra were recorded with a Tecmag Redstone spectrometer (Tecmag Inc., Texas, USA). The NMR magnet is set to be in resonance with the BDPA EPR transition when irradiating at 395 GHz with the gyrotron source. Additional field sweep capabilities are provided by home-build sweep coils mounted on the probe. At maximum current (2 A at 3 V), they allow for a ±17 mT sweep range. As a downside, when activated, the sweep coils distort the NMR line, broadening the lines inhomogeneously and reducing the sensitivity (Fig. S7, SI).

Enhancements were estimated by taking the ratio of integrals of the NMR signal under microwave (MW) irradiation (MW ON, $I_{MW\text{-}ON}$) and at thermal equilibrium (MW OFF, $I_{MW\text{-}OFF}$), *i.e.* $\varepsilon \sim I_{MW\text{-}ON}/I_{MW\text{-}OFF}$. To control the temperature rise due to the MW irradiation, the sample is under a constant flow (25 L min^{-1}) of cold nitrogen gas ($T_{gas} \sim -5$ to -30 °C, depending on the freezing point of the sample).[5,43] To further limit the heating effect, the MW irradiation was limited to 4 s prior to the NMR detection, and the recycle delay between consecutive scans was set at 12 s to allow for a cooling phase. To exclude that temperature effects influence the estimation of the enhancements, we checked that the enhancement when irradiating off-resonance of the EPR transition (*i.e.* when no enhancement is expected) is $\varepsilon_{off\text{-}Res} \sim (I_{MW\text{-}ON}/I_{MW\text{-}OFF})_{off\text{-}Res} \sim 1$. When this condition was not met, we considered the ratio of the peak integrals recorded on-resonance with the EPR transition and off-resonance of the EPR transition, both recorded with MW ON, *i.e.* $\varepsilon \sim (I_{MW\text{-}ON})_{on\text{-}Res}/(I_{MW\text{-}ON})_{off\text{-}Res}$.

Results and discussion

Radical persistence

The persistence of the radicals in powder form was monitored over a period of ~30 days by measuring EPR spectra under the same experimental conditions (Fig. 1b). For each spectrum, we calculated the double integral, which is proportional to the number of spins in the sample and therefore to the radical content. Powder samples were stored in a −80 °C freezer in between measurements. BDPA (in a 1 : 1 complex with benzene, see Materials and methods), verdazyl, and galvinoxyl in powder form show a modest decay over a 30 day period, losing ~10% of their initial radical content. For BDPA, we conducted additional experiments by storing the samples at ambient conditions (*bench*) or in a glovebox (Fig. S1, SI). Our data show that the modest decay rate of BDPA in powder is unaffected by the storage conditions.

In contrast with the other radicals tested, PF-trityl exhibits a higher depletion rate in powder when stored in a −80 °C freezer (Fig. 1), and the spin count decreases by ~40% in 20 days. The decay is driven by oxygen and photodecomposition; storing PF-trityl at low temperatures in an inert environment in the dark (*e.g.* a freezer inside a glovebox or in a flask under vacuum stored in a freezer) may improve the persistence of the radical.[46,47]

The persistence of organic radicals in solution was measured by performing CW-EPR over >20 days in solutions of *p*-xylene and CCl_4, with radical concentrations in the range 10–40 mM (Fig. 2). Among the tested radicals, we included TEMPO because it has been extensively and effectively used as PA for ^{13}C-DNP.[4,48] To assess the reproducibility of the these experiments, we repeated measurements on a few samples to rule out any outside effects that could alter our assessment of the persistence of radical in solution, *e.g.* sample leaking (Fig. S4, SI). The error on the EPR data presented in this section is estimated at 15%.

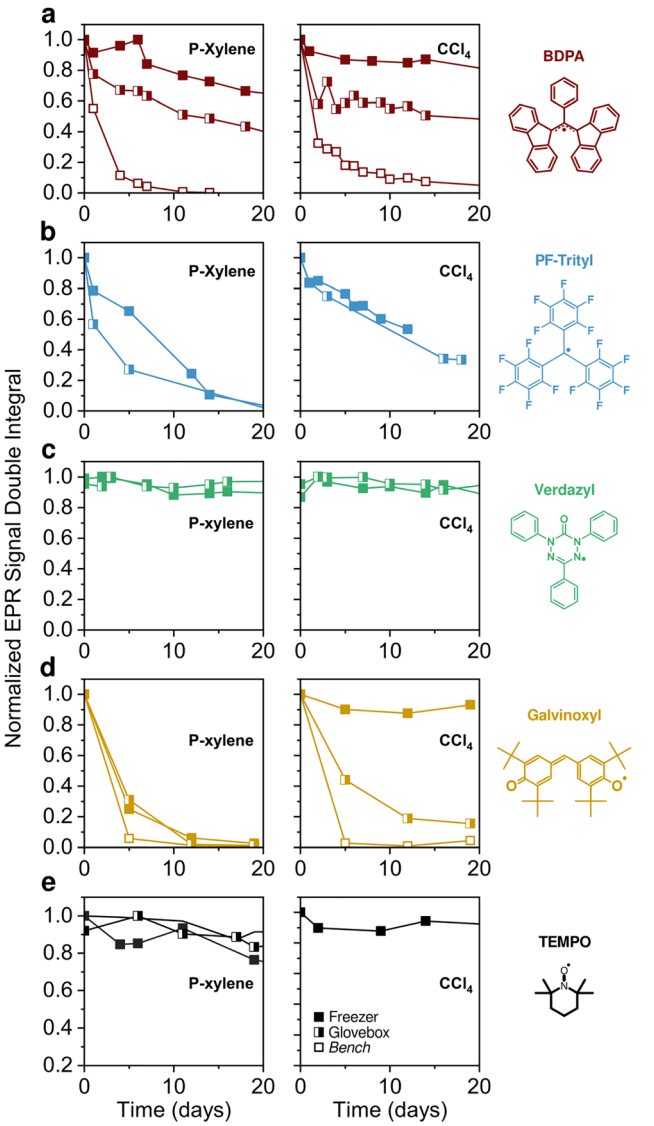


Fig. 2 Persistence of (a) BDPA, (b) PF-trityl, (c) verdazyl, (d) galvinoxyl, and (e) TEMPO radicals in solutions of CCl_4 and *p*-xylene evaluated with CW-EPR. Storage conditions in between measurements are: *freezer* (filled squares), *glovebox* (half-filled squares), *bench* (empty squares). All samples were degassed. Note: Line segments are connecting experimental data points. Error bars (15%) are omitted for clarity. For clarity, decays are displayed up to day 20, while the full data sets are shown in Fig. S6 in the SI.

Nitrogen-based radicals like verdazyl and TEMPO have the highest persistence over time among the tested radicals in all storage conditions and in both tested solvents, with a radical decay of ≤20% over ~20 days (Fig. 2c and e).

The persistence of carbon-based radicals (BDPA, PF-trityl, and galvinoxyl) varies significantly depending on the type of monoradical, the solvent, and the storage condition. The persistence of BDPA is low for bench storage, with the radical content decaying down to 10% in only 4 days (Fig. 2a). A similar behavior is observed in benzene and $CHCl_3$ (Fig. S5, SI), and has also been previously reported for BDPA derivatives in H_2O and glycerol.[29] This can be ascribed to the storage environment

This journal is © the Owner Societies 2026

and the oxygen content, which can increase over time when samples are stored on the bench, given the partial porosity of FEP to O_2.[5,43] This is further confirmed by the fact that the persistence of BDPA is higher when the sample is stored in a glovebox (Fig. 2a). Storing the sample in the freezer offers the highest persistence in terms of radical content in *p*-xylene and CCl_4, as well as in benzene and $CHCl_3$ (Fig. S5, SI). While deoxygenation increases DNP performance because narrows the EPR lines and extends the electronic relaxation times, degassing the sample prior to its storage seems to slightly deteriorate the persistence of BDPA (Fig. S7, SI), though this effect requires further investigation to be confirmed and additional experiments are ongoing.

Galvinoxyl and PF-trityl are the least stable among the tested radicals (Fig. 2b and d). Galvinoxyl is sensitive to O_2, and previous results showed that the persistence in solution goes from tens of minutes to a few hours, depending on the solvent.[49] Here, the persistence of galvinoxyl is improved to a few days thanks to sample degassing (Fig. 2d). Galvinoxyl in CCl_4 showed a remarkable stability only when stored in the freezer, losing ~10% of its initial radical content (Fig. 2d). The radical decays in a few days when stored either on the bench or in the glovebox, with the latter performing only slightly better. When dispersed in *p*-xylene, galvinoxyl lost ~100% of their initial radical content regardless of the storage method (Fig. 2d). This aligns with a previous report showing that the persistence of galvinoxyl in solution under ambient conditions ranges from a few hours to approximately one day.[49]

PF-trityl showed low persistence of radical in solution regardless of the solvent used, with *p*-xylene showing a more drastic decay than CCl_4. Over a 20 day period in solution with *p*-xylene, the concentration of PF-trityl in solution lost about 95% of the initial content, while the persistence is only slightly higher when in solution with CCl_4 (Fig. 2b). Although efforts were made to screen the samples from ambient lighting during sample transport and handling, a potential contributor to PF-trityl's large decay in both *p*-xylene and CCl_4 is its photosensitivity. Fig. S2 in the SI shows that the decay of PF-trityl in solution of dichloromethane can be as fast as a few hours when exposed to ambient conditions (lighting and oxygen). In the context of DNP, variants of trityl radicals soluble in water, like OX063 or Finland, have been utilized.[1,13] The persistence of these variants can vary significantly from minutes to days depending on conditions such as pH, presence of reducing agents, or oxygen reactive species.[50,51] Some of those trityl variants can be stable for a few days in water in neutral conditions.[52] Those radicals are also prone to aggregation,[51] although we did not observe any sign of aggregation in PF-trityl in the tested conditions.

In the context of DNP in the liquid state, triphenylphosphine (PPh_3) is often used as a target molecule in combination with BDPA radical due to the large ^{31}P enhancements that are readily attainable at both low and high magnetic fields.[9,25,53,54] More recently, hyperpolarized PPh_3 has been used as a polarization reservoir to effectively polarize solid surfaces, as shown in pioneering works by Emsley and coworkers,[17,18] further solidifying PPh_3 as an important molecule in DNP.

Additionally, PPh_3 has been used as an oxygen scavenger in liquids since it efficiently removes oxygen dissolved in solution through an autoxidation process.[55] This autoxidation process involves a radical initiator and proceeds through a free-radical chain mechanism. Once this process is initiated, oxygen is continuously incorporated into radical intermediates and converted into triphenylphosphine oxide.[56]

Motivated by the lack of reproducibility we experienced when dealing with ^{31}P-DNP on PPh_3, we monitored the persistence of BDPA, PF-trityl and TEMPO in benzene upon the addition of PPh_3 (Fig. 3). The curves show that the persistence of BDPA in benzene is impacted significantly, which depletes by ~50% in the first 24 h (Fig. 3a). The radical PF-trityl decays upon the addition of PPh_3, and the EPR signal is barely detectable after the sample preparation (Fig. 3b). TEMPO does not show this trend, maintaining similar stability over a period of 20 days regardless of PPh_3 content in solution (Fig. 3b). The reason for this accelerated BDPA depletion has not been investigated further.

Radical persistence in DNP

To elucidate the effect of the radical depletion in DNP in liquids, we monitored the ^{19}F enhancement as a function of time on a sample of hexafluorobenzene (HFB) (~540 mM)

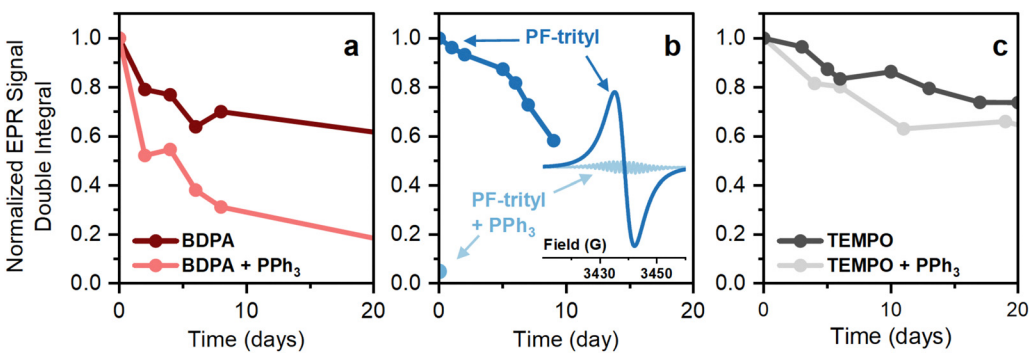


Fig. 3 Persistence monitored *via* CW-EPR of (a) BDPA, (b) PF-trityl, and (c) TEMPO radicals in solution of benzene with and without the addition of PPh_3. Samples were degassed and stored in a −80 °C freezer in between measurements. The inset in panel (b) shows the EPR spectra of PF-trityl without (dark blue) and with (light blue) PPh_3 at day 0, right after sample preparation. Decays are displayed up to day 20, while the full data sets are shown in Fig. S8 in the SI.

doped with BDPA (~10 mM) dissolved in *p*-xylene. Fig. 4 shows the correlation between the radical content and the ^{19}F enhancements at 14.1 T. While stored in a glovebox at room temperature in between measurements, the radical content decayed by ~20% in 17 days (Fig. 4a); over the same time period, the enhancement shows a steep decrease from $\varepsilon_{\text{day }0} \sim 10$ to $\varepsilon_{\text{day }17} \sim 5$. The radical depletion is exacerbated when the sample is stored at room temperature and ambient conditions (*bench*): from day 18 to 20, the radical concentration is reduced to ~2 mM, about 20% of the original one, as evident by the sudden large drop in EPR signal intensity (Fig. 4a). Consequently, the enhancement at day 20 is not observable (Fig. 4c). A similar behaviour was observed for PF-trityl (Fig. 4d–f), although on a faster timescale. Starting at 30 mM, the radical decays by 20% in 5 days, although stored in the freezer and under inert conditions; after this, PF-trityl was exposed to ambient condition for 12 hours, the radical concentration went down to 10 mM, and no enhancement is observed.

Finally, we note that the microwave irradiation and consequent temperature increase on the sample seems not to affect the BDPA persistence in solution. In fact, the EPR spectra of BDPA recorded before and after about 1 hour of continuous DNP experiments (50 scans with 20 s of MW irradiation, 60 s recycle delay) show no significant difference (Fig. S9, SI).

New polarizing agents for DNP at 14.1 T

While BDPA, TEMPO, and galvinoxyl have been previously utilized as PAs at both low and high magnetic fields, PF-trityl and verdazyl are new in the context of high-field DNP in the liquid state. In Fig. 5, we show the OE-DNP enhancements obtained at 14.1 T with PF-trityl (Fig. 5a) and verdazyl (Fig. 5b). As target molecules, we utilized HFB and perfluorinated hexene (PF-hexene), here used as model systems to showcase the DNP performance on both aromatic and aliphatic fluorinated compounds. Previous studies showed that carbon-based radicals such as galvinoxyl and BDPA exhibit a more efficient polarization transfer to aromatic compounds, potentially favoured by radical-target compound plane-to-plane interactions that resemble π-stacking.[5,25,57]

Since the electron spin of different radicals resonates at different field positions, we measured the CW-EPR spectra of PF-trityl and verdazyl in solution at 240 GHz (SI Fig. S3). The *g*-values are $g_{\text{iso}} \sim 2.0030$ for PF-trityl and $g_{\text{iso}} \sim 2.0035$ for verdazyl in reference to BDPA ($g_{\text{iso}} = 2.0025$). At 14.1 T and 395 GHz, PF-trityl resonates at about −3.5 mT with respect to the BDPA, while verdazyl resonantes at about −7 mT. Both resonances are reachable using the additional sweep coils mounted on the DNP probe. Although the probe can achieve a resolution of 0.1 ppm for ^{19}F lines, field inhomogeneities introduced by activating the sweep coils broaden these lines by a factor of 3–4 (Fig. S10, SI), ultimately reducing sensitivity. This limitation does not affect the overall DNP performance because it has a minor impact on the EPR line, which spans >100 ppm in units of ^{19}F chemical shift (Fig. S10, SI). This issue could be avoided by directly shifting the main static magnetic field rather than utilizing probe sweep coils, which is a more time-consuming process. Alternative probe designs can

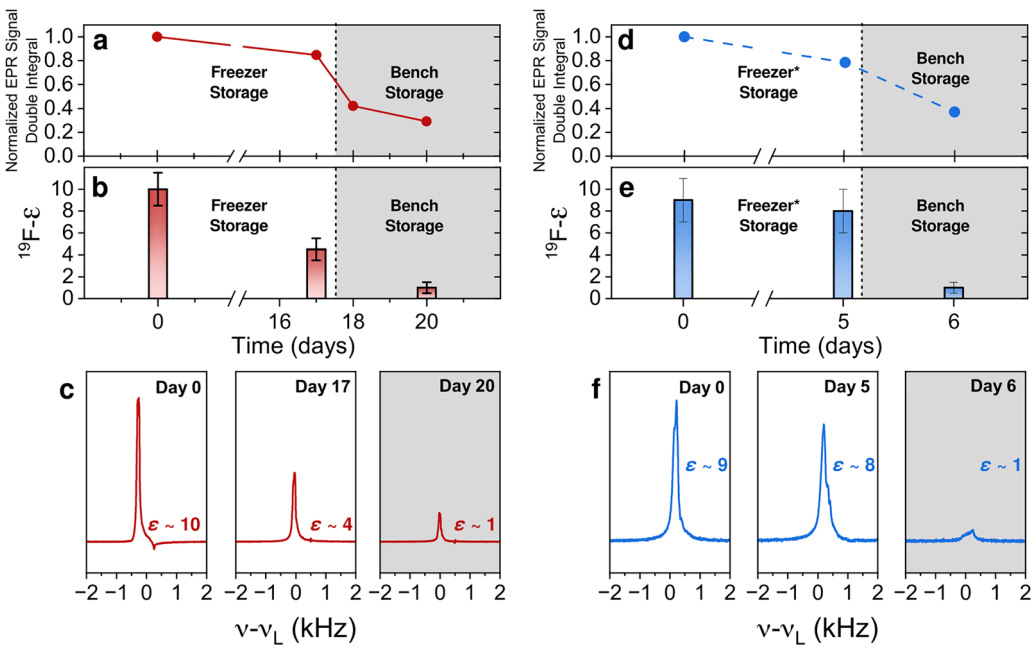


Fig. 4 (a) Persistence of BDPA radical (10 mM) in a solution of HFB (540 mM) and *p*-xylene. The sample was degassed and sealed as described in the Materials and methods section. (b) Corresponding ^{19}F enhancements obtained on HFB obtained at day 0, day 17, and day 20 as counted from the day of sample preparation. The storage condition was changed after day 17, as indicated in the figure. (c) ^{19}F-NMR spectra of HFB obtained under MW irradiation. (d) Persistence of PF-triyl radical (30 mM) in a solution of fluorobenzene (1.5 M) and *p*-xylene. The sample was degassed and sealed as described in the Materials and methods section. (e) Corresponding ^{19}F enhancements obtained on fluorobenzene obtained at day 0, day 5, and day 6 as counted from the day of sample preparation. The storage condition was changed after day 5, as indicated in the figure. (f) ^{19}F-NMR spectra of fluorobenzene obtained under MW irradiation. *The sample was stored frozen and under an inert atmosphere in between measurements.

This journal is © the Owner Societies 2026

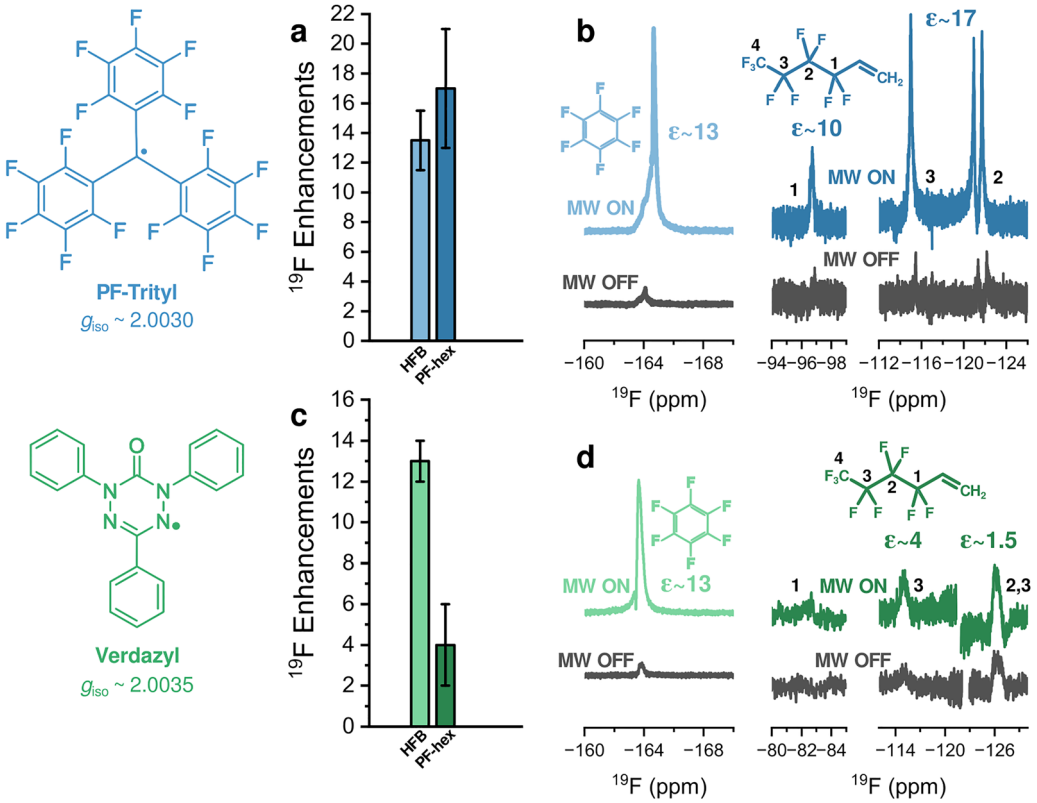


Fig. 5 ^{19}F-DNP enhancements on HFB and PF-hexene obtained with (a) and (b) PF-trityl and (c) and (d) verdazyl as polarizing agents. All samples are diluted in *p*-xylene, except for HFB + PF-trityl which is diluted in CCl_4. All samples are degassed and sealed in FEP tubes. The radical concentration is 15–25 mM, and HFB or PF-hexene concentrations are 540 mM. For comparison, under the same experimental conditions, BDPA radical leads to $\varepsilon \sim 10$ (Fig. 4), which is lower than the value of $\varepsilon \sim 37$ reported previously;[5] we attribute this discrepancy to the different concentration of BDPA (40 mM instead of the 10 mM used here) and a different degassing procedure relies on long deoxygenation of the solvents (~3 weeks) in the glovebox. Acquisition parameters: all spectra were recorded with a Hahn echo detection with 4-step phase cycling, preceded by a 4 s microwave irradiation and a presaturation block. The repetition time was set at 12 s. The number of scans was set at 4 for HFB (plus 2 dummy scans), while 100 scans and 200 scans were necessary for PF-hexene doped with PF-trityl and verdazyl, respectively. Receiver gain was kept at 50, unchanged throughout measurements.

reach linewidths of 0.03 ppm for ^{19}F (~10 Hz at 9.4 T), albeit without integrated sweep coils.[4,12]

Fig. 5a and b shows that PF-trityl leads to similar enhancements for aromatic and aliphatic fluorinated compounds, *i.e.* $\varepsilon \sim 13$ on HFB and up to $\varepsilon \sim 17$ on PF-hexene. In contrast to PF-trityl, verdazyl leads to $\varepsilon \sim 13$ for HFB, while the enhancement on the aliphatic PF-hexene is significantly lower, and does not go beyond $\varepsilon \sim 4$ (Fig. 5c and d).

Compared to verdazyl and the previously reported BDPA and galvinoxyl,[5,12] our findings suggest that PF-trityl is uniquely capable of effectively polarizing aliphatic fluorinated compounds as well as aromatic ones. While the underlying mechanism remains under investigation, we hypothesize that the ^{19}F atoms on the PF-trityl may function as polarization mediators in the intermolecular electron–nuclear spin polarization transfer.

Conclusions

In this manuscript, we studied the persistence of narrow-line radicals commonly used in DNP in liquids. Our results show that nitrogen-based radicals (TEMPO and verdazyl) have the highest persistence in both powders and solutions, with decays limited to ≤20% over 20 days. This is independent of storage conditions, solvent, and deoxygenation.

The persistence of carbon-based radicals (BDPA, PF-trityl, and galvinoxyl) is largely dependent on solvent and storage conditions. Among those, BDPA showed an increased persistence in solution when stored in the freezer but showed notable instability when stored in the glovebox and on the bench. In comparison, PF-trityl and galvinoxyl show a persistence of only a few days in solution, limited by photodecomposition and oxygen sensitivity, respectively. In general, we found that storing samples for DNP in liquids in a freezer and possibly in inert conditions may prolong the persistence of radical content.

Finally, we evaluated the OE-DNP performance at 14.1 T of PF-trityl and verdazyl, which are new as polarizing agents for high field OE-DNP in liquids. Most notably, we found that PF-trityl is a very efficient polarizing agent capable of transferring spin polarization to both aromatic and aliphatic fluorinated molecules, a feature not observed with other radicals. Although the mechanism was not investigated here, we hypothesise that the presence of ^{19}F nuclei both on the radical and on the target molecule may favor the spin polarization transfer to fluorinated target molecules.

Author contributions

TO conceived and supervised the study; JC and LD synthesized the PF-trityl radical and characterized the compound; SK and SS synthesized the verdazyl radical and characterized the compound; KP and DB performed the EPR measurements and analyzed the data; TO and DB performed the DNP measurements and analyzed the data; TO wrote the original draft; all authors contributed to editing the manuscript.

Conflicts of interest

The authors declare no conflict of interest.

Data availablility

The data supporting this article have been included as part of the supplementary information (SI). Supplementary information incudes synthesis of verdazyl radical; CW-EPR spectra at 240 GHz; additional CW-EPR data on radical persistence; NMR line broadening; DNP field profiles. See DOI: https://doi.org/10.1039/d6cp03024f.

Acknowledgements

Work performed at the National High Magnetic Field Laboratory (NHMFL) is supported by the National Science Foundation (NSF DMR-2128556) and the State of Florida. This research was also supported by Florida State University with the CRC SEED grant no 046984 (TO). The support of the NSF CHE-2320338 grant is also acknowledged for funding the Bruker Elexys E580. Olugbeminiyi Odewole (Florida State University) is acknowledged for helping with CW-EPR measurements and sample preparation. We acknowledge Frederic Mentink-Vigier (National High Magnetic Field Laboratory) for helpful discussions.

References

1 J. Eills, D. Budker, S. Cavagnero, E. Y. Chekmenev, S. J. Elliott, S. Jannin, A. Lesage, J. Matysik, T. Meersmann, T. Prisner, J. A. Reimer, H. Yang and I. V. Koptyug, Spin Hyperpolarization in Modern Magnetic Resonance, *Chem. Rev.*, 2023, **123**, 1417–1551.

2 L. Yang, I. Tkach, A. Van Der Ham, M. Reinhard, Y. Rao, T. Wolf, I. Kuprov, M. Levien, T. Orlando and M. Bennati, Recent progress in high-field liquid-state Overhauser dynamic nuclear polarization, *Prog. Nucl. Magn. Reson. Spectrosc.*, 2026, **154–155**, 101600.

3 D. Dai, X. Wang, Y. Liu, X. Yang, C. Glaubitz, V. P. Denysenkov, X. He, T. Prisner and J. Mao, Room-temperature dynamic nuclear polarization enhanced NMR spectroscopy of small biological molecules in water, *Nat. Commun.*, 2021, **12**, 6880.

4 M. Levien, L. Yang, A. van der Ham, M. Reinhard, M. John, A. Purea, J. Ganz, T. Marquardsen, I. Tkach, T. Orlando and M. Bennati, Overhauser enhanced liquid state nuclear magnetic resonance spectroscopy in one and two dimensions, *Nat. Commun.*, 2024, **15**, 5904.

5 S. Wi, J. Lumata, T. Dubroca, T. Orlando and L. Frydman, 14.1 T Liquid-State ^{19}F Overhauser Dynamic Nuclear Polarization in an Analytical Organic Setting, *J. Am. Chem. Soc.*, 2026, **148**, 20064–20075.

6 V. P. Denysenkov and T. F. Prisner, Liquid-state Overhauser DNP at High Magnetic Fields, *eMagRes*, 2019, **8**, 41–54.

7 M. Bennati and T. Orlando, Overhauser DNP in liquids on ^{13}C nuclei, *eMagRes*, 2019, **8**, 11–18.

8 P. Neugebauer, J. G. Krummenacker, V. P. Denysenkov, C. Helmling, C. Luchinat, G. Parigi and T. F. Prisner, High-field liquid state NMR hyperpolarization: a combined DNP/NMRD approach, *Phys. Chem. Chem. Phys.*, 2014, **16**, 18781–18787.

9 T. Dubroca, A. N. Smith, K. J. Pike, S. Froud, R. Wylde, B. Trociewitz, J. McKay, F. Mentink-Vigier, H. van Tol, S. Wi, W. Brey, J. R. Long, L. Frydman and S. Hill, A quasi-optical and corrugated waveguide microwave transmission system for simultaneous dynamic nuclear polarization NMR on two separate 14.1 T spectrometers, *J. Magn. Reson.*, 2018, **289**, 35–44.

10 D. Yoon, M. Soundararajan, S. Sekatski, J. Genoud, S. Alberti and J.-P. Ansermet, High-Field ^{13}C Dynamic Nuclear Polarization in Nanodiamond, *J. Phys. Chem. C*, 2019, **123**, 21237–21243.

11 T. Orlando, R. Dervişoğlu, M. Levien, I. Tkach, T. F. Prisner, L. B. Andreas, V. P. Denysenkov and M. Bennati, Dynamic Nuclear Polarization of ^{13}C Nuclei in the Liquid State over a 10 Tesla Field Range, *Angew. Chem., Int. Ed.*, 2019, **58**, 1402–1406.

12 M. Reinhard, A. van der Ham, L. Yang, L. Bröker, T. Orlando, I. Tkach, M. Levien and M. Bennati, Enhancing NMR Signals in Liquids by Fluorine-19 Overhauser Dynamic Nuclear Polarization (DNP) and Hyperpolarization Transfer to Carbon-13, *Angew. Chem., Int. Ed.*, 2025, **64**, e202517498.

13 A. A. Kuzhelev, V. Denysenkov, I. M. Ahmad, O. Y. Rogozhnikova, D. V. Trukhin, E. G. Bagryanskaya, V. M. Tormyshev, S. T. Sigurdsson and T. F. Prisner, Solid-Effect Dynamic Nuclear Polarization in Viscous Liquids at 9.4 T Using Narrow-Line Polarizing Agents, *J. Am. Chem. Soc.*, 2023, **145**, 10268–10274.

14 A. Kuzhelev, ^{31}P Dynamic Nuclear Polarization through the Solid Effect: Study of Biomolecules in Aqueous Solutions at 9.4 T, *Anal. Chem.*, 2025, **97**(28), 14890–14893.

15 O. Jakdetchai, V. P. Denysenkov, J. Becker-Baldus, B. Dutagaci, T. F. Prisner and C. Glaubitz, Dynamic nuclear polarization-enhanced NMR on aligned lipid bilayers at ambient temperature, *J. Am. Chem. Soc.*, 2014, **136**, 15533–15536.

16 A. A. Kuzhelev, D. Dai, V. P. Denysenkov and T. F. Prisner, Solid-like Dynamic Nuclear Polarization Observed in the Fluid Phase of Lipid Bilayers at 9.4 T, *J. Am. Chem. Soc.*, 2022, **144**, 1164–1168.

17 Y. Rao, F. De Biasi, R. Wei, C. Copéret and L. Emsley, Probing Homogeneous Catalysts and Precatalysts in Solution by Exchange-Mediated Overhauser Dynamic Nuclear Polarization NMR, *J. Am. Chem. Soc.*, 2024, **146**, 12587–12594.

18 Y. Rao, D. Gioffrè, M. Levien, M. Wörle, P. Pandey, M. Mazzanti, C. Copéret and L. Emsley, Surface Enhanced

 This journal is © the Owner Societies 2026

Nuclear Magnetic Resonance Spectroscopy at Solid–Liquid Interfaces Using Overhauser Dynamic Nuclear Polarization, *J. Am. Chem. Soc.*, 2025, **147**, 21297–21301.
19 C. Gabriel, S. Gabriel, E. H. Grant, B. S. J. Halstead and D. Michael P Mingos, Dielectric parameters relevant to microwave dielectric heating, *Chem. Soc. Rev.*, 1998, **27**, 213–223.
20 P. Neugebauer, J. G. Krummenacker, V. P. Denysenkov, G. Parigi, C. Luchinat and T. F. Prisner, Liquid state DNP of water at 9.2 T: an experimental access to saturation, *Phys. Chem. Chem. Phys.*, 2013, **15**, 6049–6056.
21 L. Yang, T. Orlando and M. Bennati, Halogen-Bond-Mediated ^{13}C Overhauser Dynamic Nuclear Polarization at 9.4 T, *J. Phys. Chem. Lett.*, 2025, 4505–4514.
22 A. W. Overhauser, Polarization of nuclei in metals, *Phys. Rev.*, 1953, **92**, 411–415.
23 K. H. Hausser and D. Stehlik, in *Advances in Magnetic Resonance*, ed. J. S. Waugh, Academic Press, 1968, vol. 3, pp. 79–139.
24 C. George and N. Chandrakumar, Chemical-shift-resolved ^{19}F NMR spectroscopy between 13.5 and 135 MHz: Overhauser-DNP-enhanced diagonal suppressed correlation spectroscopy, *Angew. Chem.*, 2014, **126**, 8581–8584.
25 M. Reinhard, M. Levien, M. Bennati and T. Orlando, Large ^{31}P-NMR enhancements in liquid state dynamic nuclear polarization through radical/target molecule non-covalent interaction, *Phys. Chem. Chem. Phys.*, 2023, **25**, 822–828.
26 J. S. Hyde, J. C. W. Chien and J. H. Freed, Electron–electron double resonance of free radicals in solution, *J. Chem. Phys.*, 1968, **48**, 4226–4233.
27 M. T. Türke and M. Bennati, Saturation factor of nitroxide radicals in liquid DNP by pulsed ELDOR experiments, *Phys. Chem. Chem. Phys.*, 2011, **13**, 3630.
28 S. Mandal and S. T. Sigurdsson, On the Limited Stability of BDPA Radicals, *Chem. – Eur. J.*, 2020, **26**, 7486–7491.
29 I. M. Ahmad, P. Roy, A. Kuzhelev and S. T. Sigurdsson, Tetra-substituted BDPA radicals *via* click-chemistry and application to liquid-state DNP, *Chem. Commun.*, 2026, **62**(42), 10685–10689.
30 E. Ravera, C. Luchinat and G. Parigi, Basic facts and perspectives of Overhauser DNP NMR, *J. Magn. Reson.*, 2016, **264**, 78–87.
31 G. Parigi, E. Ravera, M. Bennati and C. Luchinat, Understanding Overhauser Dynamic Nuclear Polarisation through NMR relaxometry, *Mol. Phys.*, 2019, **117**, 888–897.
32 J. R. Biller, H. Elajaili, V. Meyer, G. M. Rosen, S. S. Eaton and G. R. Eaton, Electron spin-lattice relaxation mechanisms of rapidly-tumbling nitroxide radicals, *J. Magn. Reson.*, 2013, **236**, 47–56.
33 N. Enkin, G. Liu, M. D. C. Gimenez-Lopez, K. Porfyrakis, I. Tkach and M. Bennati, A high saturation factor in Overhauser DNP with nitroxide derivatives: the role of ^{14}N nuclear spin relaxation, *Phys. Chem. Chem. Phys.*, 2015, **17**, 11144–11149.
34 J. Freed, Dynamic effects of pair correlation functions on spin relaxation by translational diffusion in liquids. II. Finite jumps and independent T1 processes, *J. Chem. Phys.*, 1978, **68**, 4034–4037.
35 D. Sezer, Computation of DNP coupling factors of a nitroxide radical in toluene: seamless combination of MD simulations and analytical calculations, *Phys. Chem. Chem. Phys.*, 2013, **15**, 526–540.
36 C. Trapp, C. Wang and R. Filler, Electron Spin Resonance Absorption in the Tris(pentafluorophenyl)methyl Radical, *J. Chem. Phys.*, 1966, **45**, 3472–3474.
37 J. Schlögl, A. R. Krappe, P. C. Fürstenwerth, A. L. Brosius, C. Fasting, K. F. Hoffmann, U. Resch-Genger, S. Eigler, S. Steinhauer and S. Riedel, Luminescent Perhalofluoro Trityl Radicals, *J. Am. Chem. Soc.*, 2025, **147**, 43105–43112.
38 E. G. Delany, S. Kaur, S. Cummings, K. Basse, D. J. D. Wilson and J. L. Dutton, Revisiting the Perfluorinated Trityl Cation, *Chem. – Eur. J.*, 2019, **25**, 5298–5302.
39 K. F. Hoffmann, D. Battke, P. Golz, S. M. Rupf, M. Malischewski and S. Riedel, The Tris(pentafluorophenyl)methylium Cation: Isolation and Reactivity, *Angew. Chem., Int. Ed.*, 2022, **61**, e202203777.
40 J. Schlögl, A. L. Brosius, A. N. Toraman, A. Wiesner, S. Steinhauer, C. Müller and S. Riedel, Halogenated Trityl Cations as Easy-to-Access Super Electrophiles, *Angew. Chem., Int. Ed.*, 2025, **64**, e202423857.
41 A. Garcés and I. Fernández, Understanding the Hydride Abstraction From Alkanes Promoted by Trityl Cations, *Eur. J. Org. Chem.*, 2026, e70624.
42 R. Milcent, G. Barbier, S. Capelle and J.-P. Catteau, New general synthesis of tetrahydro-1,2,4,5-tetrazin-3(2*H*)-one derivatives and stable 3,4-dihydro-3-oxo-1,2,4,5-tetrazin-1(2*H*)-yl radical derivatives, *J. Heterocycl. Chem.*, 1994, **31**, 319–324.
43 T. Orlando, H. Bui, J. Cabigting, N. Ibbetson, J. van Tol, T. Dubroca, X. Wang and F. Mentink-Vigier, Impact of non-polar solvents in dynamic nuclear polarization at high magnetic fields, *J. Magn. Reson.*, 2025, **375**, 107885.
44 J. Van Tol, L. C. Brunel and R. J. Wylde, A quasioptical transient electron spin resonance spectrometer operating at 120 and 240 GHz, *Rev. Sci. Instrum.*, 2005, **76**, 074101.
45 T. Dubroca, S. Wi, J. Van Tol, L. Frydman and S. Hill, Large volume liquid state scalar Overhauser dynamic nuclear polarization at high magnetic field, *Phys. Chem. Chem. Phys.*, 2019, **21**, 21200–21204.
46 A. Shibata and M. Abe, Mechanistic Insights into the Photodegradation of Trityl Radicals, *Org. Lett.*, 2026, **28**, 8413–8418.
47 H. E. Hackney, C. Y. Legault, H. M. Titi and D. F. Perepichka, Mechanism of the Photodecomposition of Stable Triarylmethyl Radicals, *Angew. Chem., Int. Ed.*, 2026, **65**, e26004.
48 M. Levien, M. Reinhard, M. Hiller, I. Tkach, M. Bennati and T. Orlando, Spin density localization and accessibility in organic radicals for liquid-state DNP efficiency, *Phys. Chem. Chem. Phys.*, 2021, **23**, 4480–4485.
49 L. Lampp, M. Azarkh, M. Drescher and P. Imming, Galvinoxyl radicals: Synthesis of new derivatives, determination of low oxygen contents, and stability studies, *Tetrahedron*, 2019, **75**, 2737–2747.

50 T. Y. Karogodina, S. V. Sergeeva and D. V. Stass, Stability And Reactivity Of Free Radicals: APhysicochemical Perspective With Biological Implications, *Hemoglobin*, 2011, **35**, 262–275.
51 U. Sanzhaeva, M. Poncelet, O. Tseytlin, M. Tseytlin, M. Gencheva, T. D. Eubank, V. V. Khramtsov and B. Driesschaert, Synthesis, Characterization, and Application of a Highly Hydrophilic Triarylmethyl Radical for Biomedical EPR, *J. Org. Chem.*, 2020, **85**, 10388–10398.
52 Z. Hasanbasri, K. Singewald, T. D. Gluth, B. Driesschaert and S. Saxena, Cleavage-Resistant Protein Labeling With Hydrophilic Trityl Enables Distance Measurements In-Cell, *J. Phys. Chem. B*, 2021, **125**, 5265–5274.
53 N. M. Loening, M. Rosay, V. Weis and R. G. Griffin, Solution-state dynamic nuclear polarization at high magnetic field, *J. Am. Chem. Soc.*, 2002, **124**, 8808–8809.
54 D. Yoon, A. I. Dimitriadis, M. Soundararajan, C. Caspers, J. Genoud, S. Alberti, E. de Rijk and J.-P. Ansermet, High-Field Liquid-State Dynamic Nuclear Polarization in Microliter Samples, *Anal. Chem.*, 2018, **90**, 5620–5626.
55 Y. Ogata and M. Yamashita, Kinetics of the autoxidation of trimethyl phosphite, methyl diphenyl-phosphinite, and triphenylphosphine, *J. Chem. Soc., Perkin Trans. 2*, 1972, 730.
56 Z. B. Alfassi, P. Neta and B. Beaver, Radiolytic Studies of the Mechanism of Autoxidation of Triphenylphosphine and Related Compounds, *J. Phys. Chem. A*, 1997, **101**, 2153–2158.
57 E. H. Poindexter, J. R. Stewart and P. J. Caplan, Dynamic polarization of fluorine nuclei in solutions of selected free radicals, *J. Chem. Phys.*, 1967, **47**, 2862–2873.

 This journal is © the Owner Societies 2026